A Simulation Study of Alkanes in Linde Type A Zeolites

Almudena García-Sánchez, Elena García-Pérez, David Dubbeldam, Rajamani Krishna and Sofía Calero

Reprinted from

Adsorption Science & Technology

2007 Volume 25 Number 6

Multi-Science Publishing Co. Ltd.
5 Wates Way, Brentwood, Essex CM15 9TB, United Kingdom

A Contribution on the Occasion of the 65th Birthday of Professor Władysław Rudziński

A Simulation Study of Alkanes in Linde Type A Zeolites

Almudena García-Sánchez[1,2], Elena García-Pérez[1], David Dubbeldam[3], Rajamani Krishna[2] and Sofía Calero[1*] *(1) Department of Physical, Chemical and Natural Systems, University Pablo de Olavide, Ctra. Utrera km. 1, 41013 Seville, Spain. (2) van't Hoff Institute for Molecular Sciences, University of Amsterdam, Nieuwe Achtergracht 166, 1018 WV Amsterdam, The Netherlands. (3) Chemical & Biological Engineering Department, Northwestern University, Evanston, IL 60208, U.S.A.*

ABSTRACT: Monte Carlo simulations were performed to study the adsorption and diffusion of small hydrocarbons in Linde Type A zeolites as a function of their calcium/sodium ratio. The diffusion studies were focused on methane whereas the adsorption simulations were performed from methane up to pentane. The results obtained showed that an increase in the number of cations in the structure (exchange of univalent sodium ions by divalent calcium ions) led to an increase in the adsorption of linear alkanes at low and medium pressure, but caused a decrease in adsorption at the highest pressures. An increase in the amount of cations favours molecular attraction and hence results in lower mobility. At higher cation loading the ions block the windows interconnecting the LTA cages, leading to a further decrease in diffusion. Methane self-diffusion coefficients obtained from our simulations were twice as high for the Linde Type 5A zeolite as for the Linde Type 4A zeolite. These results are consistent with previous experimental studies and provide a molecular picture of the influence of the zeolite type, the amount of cations contained and their location in the structure.

1. INTRODUCTION

Zeolites are crystalline aluminosilicates based on frameworks with well-defined channels and cavities. The structure consists of TO_4 (T = Si, Al) primary building units linked together by corner-sharing to form bent oxygen bridges (Meier *et al*. 1996). The presence of Al atoms induces an electrical imbalance, leading to the generation of a negatively charged framework that is compensated by additional cations. The inner surface of the zeolite can act as a catalyst. Zeolites are also widely used as water softeners (by exchanging non-framework cations with those of a nearby solution), as drying agents (anhydrous activated zeolites with a high affinity for water), for environmental clean-up and as molecular sieves in industrial separation processes (Guisnet and Gilson 2002).

Zeolites A (LTA, Linde Type A) are well-known representatives. They can crack chain paraffins catalytically and selectively to single straight-chain products and were the first zeolites used in shape-selective catalysis in 1960 (Chen *et al*. 1996). They are also used as water softeners in detergents and in horticulture, as drying agents, and as adsorbents for air and hydrocarbon

*Author to whom all correspondence should be addressed. E-mail: scaldia@upo.es.

separations. Zeolite A was first prepared by Breck and co-workers in 1956 (Breck *et al*. 1956; Reed and Breck 1956). The high silica LTA (ITQ-29) has only recently been synthesized (Corma *et al*. 2004). LTA zeolites are often synthesized in their sodium form and obey Loewenstein's rule (Loewenstein 1954). The sodium form has the chemical composition $Na_{96}Al_{96}Si_{96}O_{384}$, with a unit cell parameter of 24.555 Å and the Fm3c space group (Pluth and Smith 1980).

The structure of LTA consists of a cubic array of α-cages (diameter ≈ 11.2 Å), interconnected through eight-membered oxygen windows with a free effective diameter of ca. 4.1 Å (although this may be reduced by the presence of an exchangeable cation). The LTA unit cell is formed by eight α-cages, with each cage having 12 negative charges which must be compensated by exchangeable cations. The effective size of the windows in zeolite A can be modified by the correct choice of cations which partially block the pore windows. In such a way, pore cross-sections of 3 Å (K^+-exchanged form), 4 Å (Na^+-exchanged form) or 5 Å (Ca^{2+}/Na^+ form) can be produced. The Na^+/Ca^{2+} form (zeolite 5A) is obtained by replacing the sodium with calcium cations via a post-synthesis exchange. Although the names LTA 3A, 4A and 5A originated independently, they fortuitously coincide with windows sizes of ca. 3, 4 and 5 Å, respectively.

The Linde Type A framework contains three types of aluminosilicate rings that coordinate the cations as shown in Figure 1. LTA 4A has 12 sodium cations per α-cage distributed among three crystallographic sites [see Figure 1(a)]: eight in the centre of the six ring, three in the eight-ring window and one opposite to a four-ring window (Pluth and Smith 1980). In Linde 5A, four crystallographic sites are considered [see Figure 1(b)]: the eight-ring window, the six-ring window and two more sites displaced into either the α-cage or the sodalite unit from the centre of the six rings. In the calcium form, all six doubly-charged cations are coordinated to the six-rings and not to the eight-rings (Pluth and Smith 1983). The preference of the cations to coordinate to the six-rings is also observed in the mixed Na^+/Ca^{2+} form (Firor and Seff 1978).

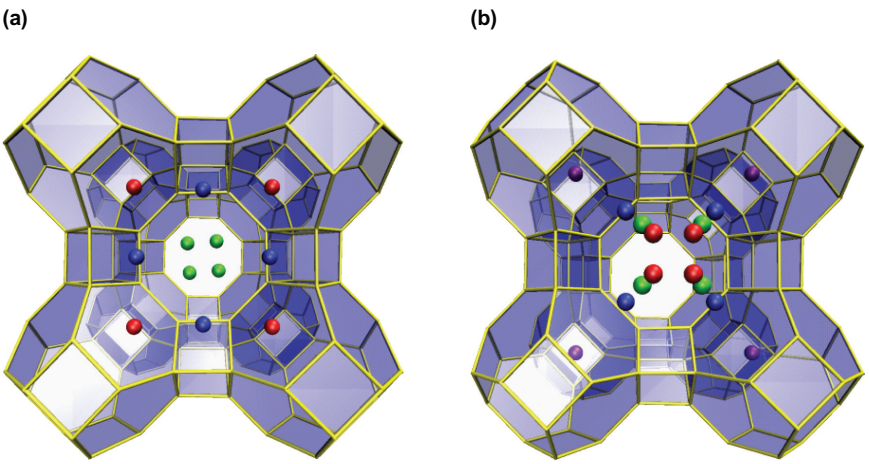

Figure 1. The Linde Type A zeolite framework contains three types of aluminosilicate rings that coordinate the cations. (a) Linde 4A has 12 sodiums per α-cage distributed among three crystallographic sites: eight in the centre of the six rings (positions in red), three in the eight-ringed window (positions in green) and one opposite to a four-ring (positions in blue). (b) Linde 5A has four crystallographic sites for cations: the eight-ringed window (positions in red), the six-ringed window (positions in blue) and two more sites displaced into either the α-cage (positions in green) or the sodalite unit (positions in purple) from the centre of the six rings.

The distribution of the cations has a significant influence on the adsorption and diffusion properties of zeolite A. Simulation studies on these systems can provide a better understanding of the effect of the Na^+/Ca^{2+} ratio, thereby leading to the control of molecular adsorption and diffusion in LTA zeolites through tuning the Na^+/Ca^{2+} ratio. A variety of simulation studies has been undertaken for the *pure silica* structure on adsorption and diffusion (Bates *et al*. 1996; Beerdsen *et al*. 2004, 2006a,b; Dubbeldam *et al*. 2006; Dubbeldam and Smit 2003; Fritzsche *et al*. 1994, 1996, 1998, 2000; Maesen *et al*. 2006; Schuring *et al*. 2002, 2004; Tunca and Ford 2003), but only a few papers have reported simulations of adsorption in LTA 4A and 5A with sodium and calcium cations (Daems *et al*. 2007; García-Pérez *et al*. 2006; Jaramillo and Chandross 2004) and we are not aware of simulation studies of diffusion in these systems.

In the present work, we provide new insights into the effect that the Na^+/Ca^{2+} ratio exerts on the adsorption and diffusion of hydrocarbons in LTA 4A and 5A. The remainder of the paper is organized as follows. In Section 2, we present our simulation methods including descriptions of the force fields used in this work. In Section 3, we continue with the simulation results and finally in Section 4 we provide some concluding remarks.

2. METHODS

2.1. Zeolite model

The Linde Type A framework was constructed from silicon, aluminium and oxygen atoms using the crystallographic positions of Pluth and Smith (1980). The Si/Al ratio is exactly one, leading to an alternating arrangement of Si and Al atoms (the Loewenstein rule forbids Al–O–Al linkages). Simulations were performed for 10 structures by varying the cation ratio: $96Na^+/0Ca^{2+}$, $80Na^+/8Ca^{2+}$, $72Na^+/12Ca^{2+}$, $56Na^+/20Ca^{2+}$, $48Na^+/24Ca^{2+}$, $38Na^+/29Ca^{2+}$, $32Na^+/32Ca^{2+}$, $24Na^+/36Ca^{2+}$, $4Na^+/46Ca^{2+}$, together with the pure silica structure with $0Na^+/0Ca^{2+}$. The Na–O and Ca–O interactions were calibrated to reproduce the experimentally known positions in LTA 4A and LTA5A (Figure 1) employing the charges $q_{Na} = +1$ and $q_{Ca} = +2$. In addition, the crystallographic locations of the sites obtained through molecular simulations were within 0.2 Å from those obtained via X-ray diffraction studies (Calero *et al*. 2004; García-Pérez *et al*. 2006). The charge distribution on the oxygen framework was considered to be static, i.e. polarization of oxygen by nearby cations was neglected. We use a model that explicitly distinguishes silicon from aluminium with a difference of $0.3e^-$ between q_{Si} and q_{Al} (Jaramillo and Auerbach 1999), considering different charges for oxygen atoms bridging two silicon atoms, q_{OSi}, and oxygen atoms bridging one silicon and one aluminium atom, q_{OAl}. All partial charges are listed in Table 1. The exchangeable cation density was adjusted to match the framework aluminium density, and the density of the zeolite was determined by the framework atoms (aluminium, silicon and oxygen) and the cations (sodium and calcium). In our model, the cations can move freely and adjust their positions depending on their interactions with the framework atoms, other cations and alkane molecules. The simulations were performed using one unit cell with eight α-cages. Test simulations using eight unit cells gave identical results but were deemed too computational expensive to use with the Ewald summation for all the simulations.

2.2. Interatomic potentials

A realistic description of the interaction between the sodium and calcium cations, the zeolite framework and the alkanes is employed in this work. The interactions between guest molecules

TABLE 1. Lennard-Jones Parameters[a,b]

	O_{Si}	O_{Al}	Si	Al	Na^+	Ca^{2+}	CH_4	CH_3	CH_2
CH_4	115	115	–	–	582	590	158.5	130.84	94.21
	3.47	3.47			2.72	2.56	3.72	3.74	3.38
CH_3	93.2	93.2	–	–	443	400	130.84	108.0	77.7
	3.48	3.48			2.65	2.6	3.74	3.76	3.86
CH_2	60.5	60.5	–	–	310	440	94.21	77.7	56.0
	3.58	3.58			2.95	2.8	3.84	3.86	3.96
Na^+	23.0	23.0	–	–	–	–	582	443	310
	3.4	3.4					2.72	2.65	2.95
Ca^{2+}	18.0	18.0	–	–	–	–	590	400	440
	3.45	3.45					2.56	2.6	2.8
Charge [e^-]	q = – 1.025	q = –1.2	q = +2.05	q = +1.75	q = +1.0	q = +2.0	–	–	–

[a]ε/k_B (K) in the top left corner, σ (Å) in the bottom-right corner of each field, partial charges (e^-) of the framework sodium and calcium ions are also included. [b]All values taken from previous publications (Beerdsen *et al.* 2004; Calero *et al.* 2004; Dubbeldam *et al.* 2004b; García-Pérez *et al.* 2006).

(alkanes and cations) with the zeolite host framework were modelled by Lennard-Jones and Coulombic potentials (Calero *et al*. 2004; Dubbeldam *et al*. 2004a,b; García-Pérez *et al*. 2006). All the used parameters are listed in Table 1. The Coulombic interactions in the system were calculated using Ewald summations (Frenkel and Smit 2002). In our simulations, the convergence parameter was chosen as 0.3 with k = 9 wave vectors for high accuracy. The alkanes were described with a united atom model in which CH_x groups were considered as single interaction centres with their own effective potentials (Ryckaert and Bellemans 1978). The beads in the chain were connected by harmonic bonding potentials. The bond-bending between three neighbouring beads was modelled by a harmonic cosine bending potential, and changes in the torsional angle were controlled by a Ryckaert–Bellemans potential. The beads in a chain separated by more than three bonds interacted with each other through a Lennard-Jones potential. The van der Waals interactions between silicon atoms were taken into account through an effective potential with only the oxygen atoms of the zeolite (Bezus *et al*. 1978; Kiselev *et al*. 1985; Vlugt *et al*. 1999) and an "average" polarization was included implicitly in the parameterization by means of the polarization induced by the cation on the zeolite and by the cation on the alkanes (Calero *et al*. 2004). It should be noted that effective Lennard-Jones potentials implicitly include, in an average sense, many-body interactions (polarization), the contributions arising from instantaneous dipole–quadrupole and quadrupole–quadrupole interactions, flexibility of the framework, etc. The flexibility of the framework has a minor effect on the adsorption of small alkanes (Vlugt and Schenk 2002).

2.3. Simulation techniques

The adsorption isotherms of alkanes were computed using Configurational Bias Monte Carlo (CBMC) simulations in the Grand Canonical ensemble (Frenkel and Smit 2002). In CBMC simulations, molecules are grown segment by segment, avoiding overlap. For each segment, a set of trial orientations is generated. One of the trial positions is selected according to the Boltzmann weight of the external energy, and this selected trial orientation is added to the chain. The procedure is repeated until the entire molecule has been grown. The rules for acceptance or rejection of a grown molecule are chosen in such a way that they exactly remove the bias caused by this growing scheme. Simulations are performed in cycles and in each cycle one move is chosen at random with a fixed probability of performing a molecule displacement (0.15), rotation around the centre of mass (0.15), exchange with the reservoir (0.55) and partial re-growth of a molecule (0.15). The maximum translational and rotational displacements are adjusted to achieve an acceptance probability of 50%. The number of cycles for methane and ethane was 2×10^7 and at least 3×10^7 for propane, butane and pentane. The total number of cations remains constant during simulations. To sample cation motions, we used displacements and insertions at new randomly selected positions that bypass energy barriers.

Self-diffusion coefficients were computed using MD simulations. In such simulations, successive configurations of the system are generated by integrating Newton's laws of motion, which then yields a trajectory that describes the positions, velocities and accelerations of the particles as they vary with time. The Verlet integration scheme with a time-step of 0.5 fs was used, providing a relative energy drift smaller than 10^{-4}. Simulations were performed using the NVT ensemble. Simulations using the NVE ensemble gave equivalent results. More details can be found in Dubbeldam *et al*. (2005a). The self-diffusion coefficients are computed by taking the slope of the mean-squared displacement at extended times (Dubbeldam *et al*. 2005b, 2006).

3. RESULTS AND DISCUSSION

The effect of exchanged cations on the adsorption and diffusion behaviour of alkanes in Linde Type A zeolites has also been studied. This behaviour is strongly dependent on the amount and distribution of the sodium and calcium cations in the structure. Adsorption isotherms were computed for methane [Figure 2(a)], ethane [Figure 2(b)], propane [Figure 2(c)], butane [Figure 3(a)] and pentane [Figure 3(b)] at 273 K in LTA structures where the amounts of calcium and sodium cations were varied. Available experimental data at that temperature are included for comparison. Although much scatter exists between the experimental data of various authors, the experimental data are in overall very good agreement with our previous simulations for methane up to octadecane (Loughlin *et al*. 1990; Ruthven and Loughlin 1972). Our simulations show that the lowest adsorption corresponds to the lowest density of cations ($4Na^+/46Ca^{2+}$), while the highest adsorption corresponds to the highest density of cations ($96Na^+/0Ca^{2+}$). Adsorption follows the opposite behaviour at high pressures, with the saturation capacities being roughly independent of the amount of exchanged cations. The adsorption isotherm for the pure silica structure was also computed showing that (1) the pressure necessary to attain a particular loading

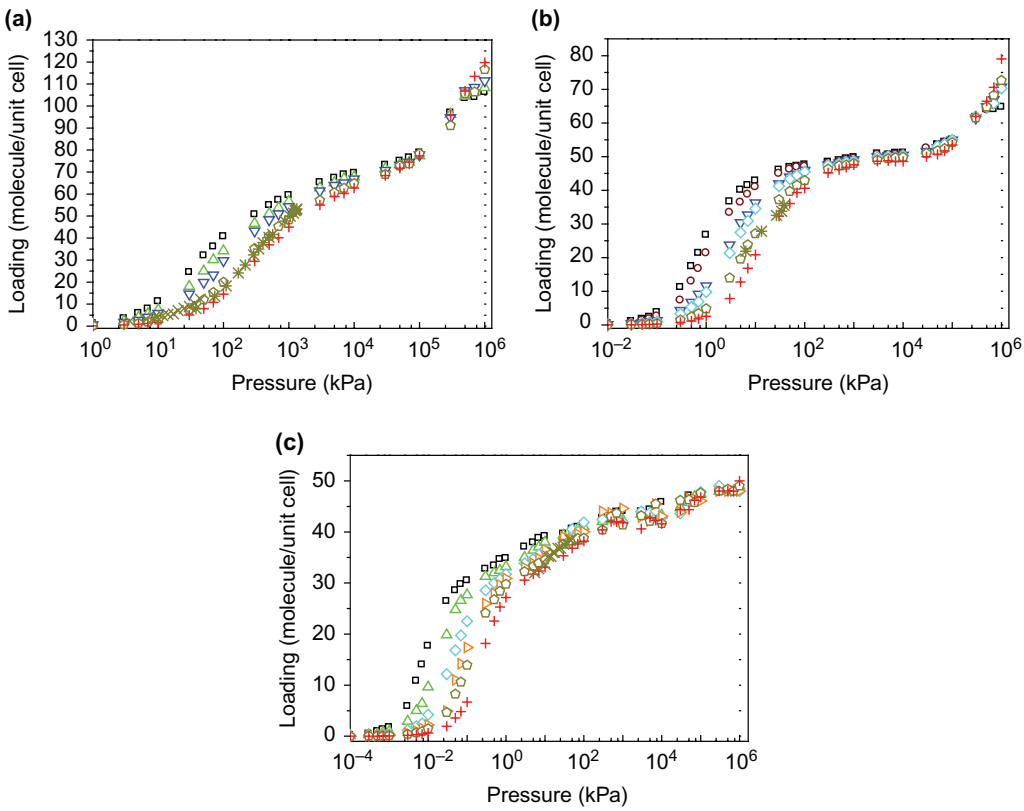

Figure 2. Adsorption isotherms of (a) methane, (b) ethane and (c) propane at 273 K in Linde Type A zeolites: (□) $96Na^+/0Ca^{2+}$; (○) $80Na^+/8Ca^{2+}$; (△) $72Na^+/12Ca^{2+}$; (▽) $56Na^+/20Ca^{2+}$; (◇) $48Na^+/24Ca^{2+}$; (▷) $32Na^+/32Ca^{2+}$; (⌒) $24Na^+/36Ca^{2+}$; and (+) $4Na^+/46Ca^{2+}$. Experimental data for the structure $24Na^+/36Ca^{2+}$ (Loughlin *et al*. 1990; Ruthven and Loughlin 1972) are included for comparison purposes: (×) Ruthven at 273 K; (✳) Loughlin at 273–275 K.

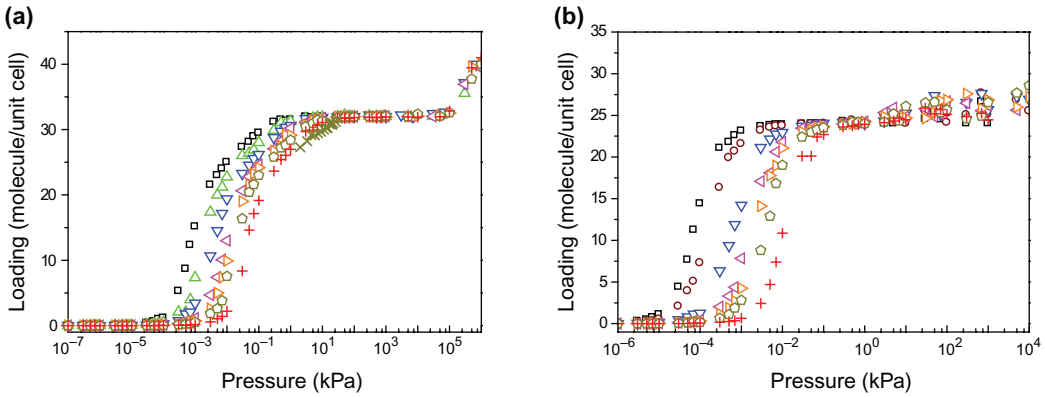

Figure 3. Adsorption isotherms of (a) butane and (b) pentane at 273 K in Linde Type A zeolites: (□) $96Na^+/0Ca^{2+}$; (○) $80Na^+/8Ca^{2+}$; (△) $72Na^+/12Ca^{2+}$; (▽) $56Na^+/20Ca^{2+}$; (◁) $38Na^+/29Ca^{2+}$; (▷) $32Na^+/32Ca^{2+}$; (◠) $24Na^+/36Ca^{2+}$; and (+) $4Na^+/46Ca^{2+}$. Experimental data for the structure $24Na^+/36Ca^{2+}$ (Ruthven and Loughlin 1972) are included for comparative purposes: (×) Ruthven at 273 K.

in the structure in the absence of cations was up to three orders of magnitude higher than that necessary for the structure containing cations and (2) the saturation loading in the pure silica structure was similar to those obtained with structures containing cations.

The explanation for this behaviour is that the cations create additional adsorption sites and also occupy free volume. The first effect dominates at low and intermediate loadings of zeolite A. We also computed the void fraction of a structure with and without cations ($32Na^+/32Ca^{2+}$) probed with a helium atom and found that the excluded volume effect is small. Thus, the void fractions were 0.39 and 0.38 for the structure devoid of cations and the cation-loaded structure, respectively. Note that the sodalite cages were blocked for helium but not for cations. The cations are not randomly located in the cages, but are well-ordered and "buried" inside the six-membered rings of the $32Na^+/32Ca^{2+}$ structure. We would like to highlight that both the cation density and the location of the cation are vital factors during the adsorption and the diffusion of alkanes in the structure. Differences of up to three orders of magnitude in adsorption were also observed in our previous studies (Calero *et al*. 2004) in all silica and sodium faujasites (another type of cage-like zeolite), where we also demonstrated that the mobility of cations is indispensable to allowing a correct reproduction of the adsorption of alkanes in aluminosilicates. The use of frozen cations leads to an over-estimation of the adsorption at low pressures and an under-estimation of the adsorption at high pressures.

Figure 4 plots the adsorption of methane and propane as a function of the sodium and calcium cation densities at a given pressure. Figure 4(a) shows that at 100 kPa the adsorption of methane and the density of sodium or calcium cations in the structure show a linear dependence. However, this linearity is not conserved at lower pressures where the trend becomes polynomial. The adsorption of propane as a function of cation density also demonstrates polynomial behaviour at several pressures as shown in Figure 4(b) for 0.01 kPa and 0.1 kPa. We have observed similar trends for ethane, butane and pentane.

The adsorption of alkanes in the zeolite was found to influence the location of the non-framework cations even at low loadings. Figure 1(b) depicts the four crystallographic sites for the cations in empty zeolite 5A (without adsorbed molecules): site 1 is in the six-ring window, sites 2 and 3 are displaced into either the α-cage or the sodalite unit from the centre of the six rings, and

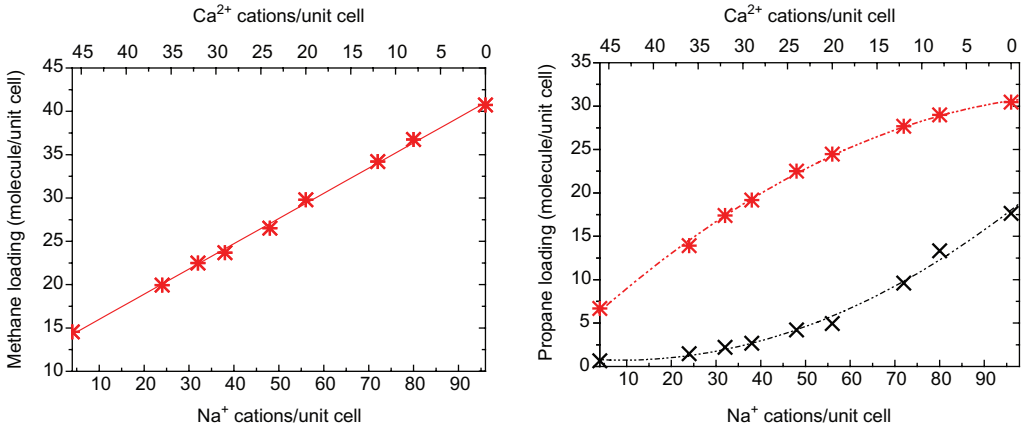

Figure 4. Amount of alkane adsorbed as a function of the sodium and calcium ion densities: (a) methane at 10^2 kPa, (b) propane at 10^{-2} kPa (×) and 10^{-1} kPa (✳).

site 4 is in the eight-ring window. Crystallographic studies indicate that the cations in zeolite 5A are only near to the six-ring windows (sites 1, 2 and 3) and not to the eight-ring window (Pluth and Smith 1983). This is in agreement with our simulations that yield occupations of 87.7% (site 1), 3.3% (site 2) and 9% (site 3). Figure 5 shows some snapshots of pentane in $48Na^+/24Ca^{2+}$ zeolite 5A taken from our simulations at 1, 10^3 and 10^6 kPa. The presence of alkanes in the zeolite increases the number of positions where the cations can be located (undefined sites) and even very small amount of alkanes have a pronounced effect on the location of the cations. Hence, cation occupations during the adsorption of pentane in $48Na^+/24Ca^{2+}$ zeolite 5A zeolite are 48.6% (site 1), 20.8% (site 3) and 30.6% (undefined sites) for 1 kPa, 79.1% (site 1), 8.3% (site 3) and 12.5% (undefined sites) for 10^3 kPa, and 80.2% (site 1), 14.3% (site 3) and 5.5% (undefined sites) for 10^6 kPa.

The adsorption isotherms of methane, ethane, propane, butane and pentane have also been compared, and the resulting simulation data for $48Na^+/24Ca^{2+}$ 5A zeolite are shown in Figure 6. Adsorption of two molecules per α-cage (16 molecules/unit cell) requires a pressure of 0.002 kPa for pentane, 0.01 kPa for butane, 0.05 kPa for propane, 2 kPa for ethane and 50 kPa for methane, At around 10^3 kPa, every α-cage adsorbs on average 3, 4, 5, 6 and 7 molecules of C_5, C_4, C_3, C_2 and C_1, respectively.

The diffusion coefficients of methane have been computed from the slope of the mean-squared displacement at long times in silica, LTA 5A ($32Na^+/32Ca^{2+}$) and LTA 4A ($96Na^+/0Ca^{2+}$). The 96 molecules of methane per unit cell at 500 K and the cations in zeolites 5A and 4A were considered as being initially located in the crystallographic positions (Pluth and Smith 1980, 1983). The computed values for the diffusion coefficients were 2.9×10^{-11} m^2/s for the *pure silica* structure, 2.4×10^{-11} m^2/s for $32Na^+/32Ca^{2+}$ zeolite 5A and ca. 3×10^{-14} m^2/s for $96Na^+/0Ca^{2+}$ zeolite 4A. Diffusion coefficients are much lower in zeolite 4A than in 5A due to the distribution of the cations. Diffusive hopping processes take place through the eight-ringed windows. In zeolite 5A none of the windows are blocked by a cation, with a free diameter for the window of 5 Å. Zeolite 4A contains 12 sodium cations per α-cage and all the windows are occupied with a cation, reducing the effective size to 4 Å. To show the influence of the cations, we performed additional simulations by placing the sodium and calcium cations at random starting positions in the $32Na^+/32Ca^{2+}$ zeolite 5A. These simulations provided a diffusion coefficient of

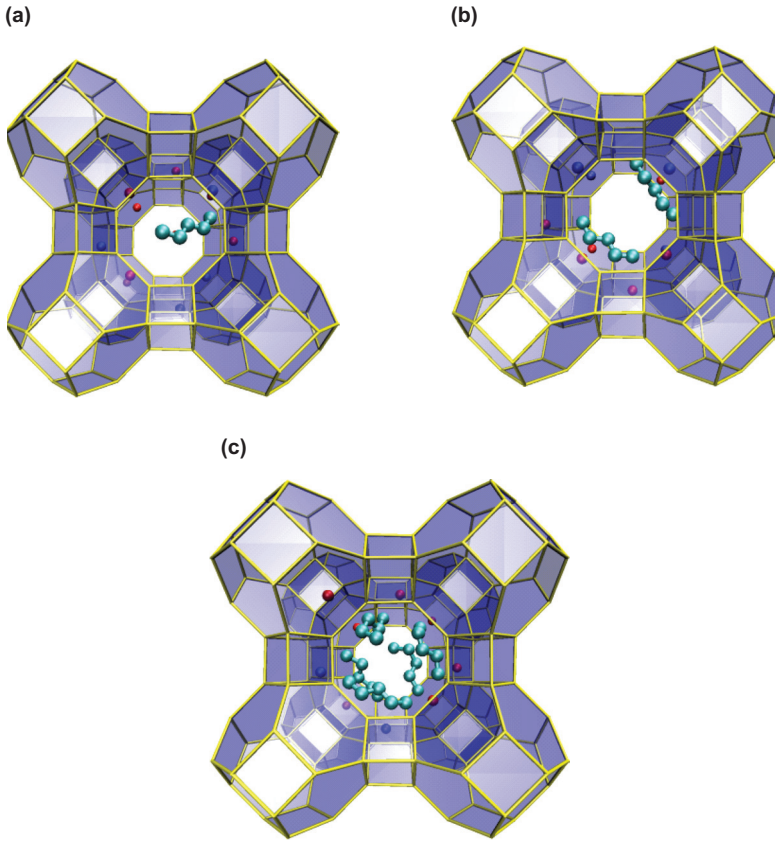

Figure 5. Snapshots of the adsorption of pentane in $48Na^{+}/24Ca^{2+}$ 5A zeolite at 273 K and (a) 1 kPa, (b) 10^3 kPa and 10^6 kPa.

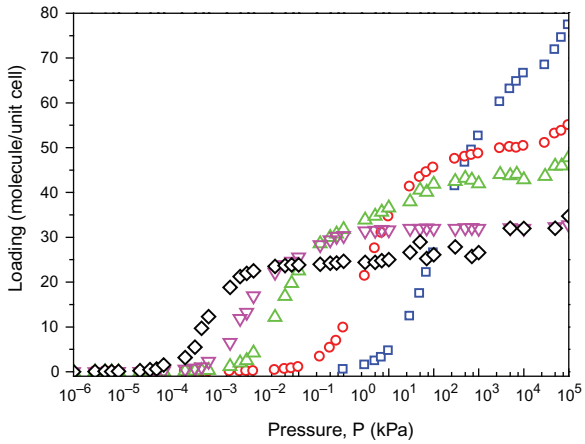

Figure 6. Adsorption isotherms of (□) methane, (○) ethane, (△) propane, (▽) butane and (◇) pentane in $48Na^{+}/24Ca^{2+}$ 5A zeolite at 273 K.

1.1×10^{-11} m^2/s, which is a clear indication that part of the windows were blocked by the randomly located cations.

4. CONCLUSIONS

We have performed a computational study of the effect of exchanged sodium and calcium cations on the adsorption and diffusion of alkanes in Linde Type A zeolites. We have demonstrated that the density and the location of cations induce marked variations in the alkane adsorption properties, and also that the adsorption of alkanes in the zeolite induces re-locations of the cations in the structure even at low loadings. During adsorption, the increase in the number of exchanged cations leads to higher loadings at low pressures and to lower loadings at high pressures. Diffusion is mostly influenced by the spatial distribution of the cation. It is slower in LTA zeolite 4A than in LTA zeolite 5A since the eight-ringed windows are partially blocked in the former and unoccupied in the later.

ACKNOWLEDGEMENTS

This work is supported by the Spanish "Ministerio de Educación y Ciencia" (CTQ2007-63229/BQU) and the National Science Foundation (CTS-0507013). The authors gratefully acknowledge the computer resources, technical expertise and assistance provided by the Barcelona Supercomputing Centre — Centro Nacional de Supercomputación. E. García-Pérez, and A. García-Sanchez wish to thank the MEC and the Netherlands Foundation for Fundamental Research (NWO-CW) for their pre-doctoral fellowships. The authors wish to thank J.M. van Baten for his useful scripts.

REFERENCES

Bates, S.P., van Well, W.J.M., van Santen, R.A. and Smit, B. (1996) *J. Am. Chem. Soc.* **118,** 6753.
Beerdsen, E., Dubbeldam, D. and Smit, B. (2006a) *J. Phys. Chem. B* **110,** 22 754.
Beerdsen, E., Dubbeldam, D. and Smit, B. (2006b) *Phys. Rev. Lett.* **96,** 44 501.
Beerdsen, E., Smit, B. and Dubbeldam, D. (2004) *Phys. Rev. Lett.* **93,** 248 301.
Bezus, A.G., Kiselev, A.V., Lopatkin, A.A. and Du, P.Q. (1978) *J. Chem. Soc., Faraday Trans. II* **74,** 367.
Breck, D.W., Eversole, W.G., Milton, R.M., Reed, T.B. and Thomas, T.L. (1956) *J. Am. Chem. Soc.* **78,** 5963.
Calero, S., Dubbeldam, D., Krishna, R., Smit, B., Vlugt, T.J.H., Denayer, J.F.M., Martens, J.A. and Maesen, T.L.M. (2004) *J. Am. Chem. Soc.* **126,** 11 377.
Chen, N.Y., Garwood, W.E. and Dwyer, F.G. (1996) *Shape Selective Catalysis in Industrial Applications*, Marcel Dekker, New York.
Corma, A., Rey, F., Rius, J., Sabater, M.J. and Valencia, S. (2004) *Nature (London)* **431,** 287.
Daems, I., Baron, G.V., Punnathanam, S., Snurr, R.Q. and Denayer, J.F.M. (2007) *J. Phys. Chem. C* **111,** 2191.
Dubbeldam, D. and Smit, B. (2003) *J. Phys. Chem. B* **107,** 12 138.
Dubbeldam, D., Beerdsen, E., Calero, S. and Smit, B. (2005a) *Proc. Nat. Acad. Sci. U.S.A.* **102,** 12 317.
Dubbeldam, D., Beerdsen, E., Calero, S. and Smit, B. (2006) *J. Phys. Chem. B* **110,** 3164.
Dubbeldam, D., Beerdsen, E., Vlugt, T.J.H. and Smit, B. (2005b) *J. Chem. Phys.* **122,** 224 712.
Dubbeldam, D., Calero, S., Vlugt, T.J.H., Krishna, R., Maesen, T.L.M., Beerdsen, E. and Smit, B. (2004a) *Phys. Rev. Lett.* **93,** 088 302.

Dubbeldam, D., Calero, S., Vlugt, T.J.H., Krishna, R., Maesen, T.L.M. and Smit, B. (2004b) *J. Phys. Chem. B* **108,** 12 301.
Firor, R.L. and Seff, K. (1978) *J. Am. Chem. Soc.* **100,** 3091.
Frenkel, D. and Smit, B. (2002) *Understanding Molecular Simulations: From Algorithms to Applications*, Academic Press, San Diego, CA, U.S.A.
Fritzsche, S., Haberlandt, R. and Wolfsberg, M. (2000) *Chem. Phys.* **253,** 283.
Fritzsche, S., Gaub, M., Haberlandt, R. and Hofmann, G. (1996) *J. Mol. Model.* **2,** 286.
Fritzsche, S., Haberlandt, R., Karger, J., Pfeifer, H. and Waldherrteschner, M. (1994) *Stud. Surf. Sci. Catal.* **84,** 2139.
Fritzsche, S., Wolfsberg, M., Haberlandt, R., Demontis, P., Suffritti, G.B. and Tilocca, A. (1998) *Chem. Phys. Lett.* **296,** 253.
García-Pérez, E., Dubbeldam, D., Maesen, T.L.M. and Calero, S. (2006) *J. Phys. Chem. B* **110,** 23 968.
Guisnet, M. and Gilson, J.-P. (2002) *Zeolites for Cleaner Technologies*, Vol. 3 in *Catalytic Science Series*, Imperial College Press, London.
Jaramillo, E. and Auerbach, S.M. (1999) *J. Phys. Chem. B* **103,** 9589.
Jaramillo, E. and Chandross, M. (2004) *J. Phys. Chem. B* **108,** 20 155.
Kiselev, A.V., Lopatkin, A.A. and Shulga, A.A. (1985) *Zeolites* **5,** 261.
Loewenstein, W. (1954) *Am. Mineral.* **39,** 92.
Loughlin, K.F., Hasanain, M.A. and Abdulrehman, H.B. (1990) *Ind. Eng. Chem., Res.* **29,** 1535.
Maesen, T.L.M., Beerdsen, E., Calero, S., Dubbeldam, D. and Smit, B. (2006), *J. Catal.* **237,** 278.
Meier, W.M., Olson, D.H. and Baerlocher, C. (1996) *Zeolites* **17,** 1.
Pluth, J.J. and Smith, J.V. (1980) *J. Am. Chem. Soc.* **102,** 4704.
Pluth, J.J. and Smith, J.V. (1983) *J. Am. Chem. Soc.* **105,** 1192.
Reed, T.B. and Breck, D.W. (1956) *J. Am. Chem. Soc.* **78,** 5972.
Ruthven, D.M. and Loughlin, K.F. (1972) *J. Chem. Soc., Faraday Trans. I* **68,** 696.
Ryckaert, J.P. and Bellemans, A. (1978) *Discuss. Faraday Soc.* **66,** 95.
Schuring, A., Auerbach, S.M., Fritzsche, S. and Haberlandt, R. (2002) *J. Chem. Phys.* **116,** 10 890.
Schuring, A., Auerbach, S.M., Fritzsche, S. and Haberlandt, R. (2004) *Stud. Surf. Sci. Catal.* **154,** 2110.
Tunca, C. and Ford, D.M. (2003) *Chem. Eng. Sci.* **58,** 3373.
Vlugt, T.J.H. and Schenk, M. (2002) *J. Phys. Chem. B* **106,** 12 757.
Vlugt, R.J.H., Krishna, R. and Smit, B. (1999) *J. Phys. Chem. B* **103,** 1102.